Hot-exciton cascades in coupled quantum wells

F. Clérot, B. Deveaud, A. Chomette, and A. Regreny
Centre National d'Etudes des Télécommunications de Lannion, 22 301 Lannion, France

B. Sermage
Centre National d'Etudes des Télécommunications de Bagneux, 92 220 Bagneux, France
(Received 14 September 1989)

By studying photoluminescence and photoluminescence excitation in coupled quantum wells, we investigate the influence of tunneling on the relaxation of photocreated carriers. The ability to vary the coupling strength between the wells by changing the tunnel-barrier thickness allowed us to study the influence of the carrier lifetime on excitation spectra. For sufficiently strong coupling, hot-exciton relaxation and resonant Raman scattering or "hot" luminescence, can be observed.

INTRODUCTION

A coupled-quantum-wells system (CQW) is a superlattice in which the period consists of a thick barrier followed by two wells of different thicknesses, separated by a thin barrier. The thick barrier isolates each set of two wells from the next one so that the system can be considered as a stack of isolated CQW's. Such a system has attracted considerable attention in recent years. Compared to isolated quantum wells, CQW's exhibit new optical properties such as interwell transfer of excitation,[1,2] interwell optical transitions,[3] and crossing of different quantized levels when subjected to an electric field,[4,5] which are now well documented.

A wide range of spectroscopic techniques has been used to study CQW's including absorption,[2,5] steady-state[1] or time-resolved[6-9] luminescence, excitation of the luminescence[10] [photoluminescence excitation (PLE)], and photoconductivity.[4]

Photoluminescence excitation and photoconductivity (PC) experiments are often expected to give the same information as absorption; however, PLE or PC spectra can show structures which are not related to the density of states, but to the energy-relaxation processes of the system. A comprehensive review of those phenomena can be found in Ref. 11 for bulk semiconductors. The basics are as follows: carriers are excited at a variable energy above the band gap and the luminescence (for PLE spectra) is detected on a line at or below the band gap. Before they can recombine radiatively, photocreated carriers must relax down to their respective band edges. If any kind of "escape mechanism," such as strong nonradiative traps, is present, the intensity of the luminescence detected for a given excitation energy will depend on the relative magnitude of the "escape time" and the time it takes for a carrier to relax down to the band edge. The same remark applies to photoconductivity experiments.

In bulk materials[12-14] or short-period superlattices[15,16] with short carrier lifetimes (due, for instance, to efficient transport towards the surface or to a high concentration of bulk nonradiative traps), PLE and PC spectra show strong resonances approximately spaced by the energy of an optical phonon. These resonances were successfully interpreted in terms of this model.

In the following we shall focus our attention on a similar phenomenon observed in PLE spectra of various CQW's. In such samples a short lifetime of the carriers in the narrow well is obtained, not as a result of the poor quality of the sample, but as a result of a short tunneling time from the narrow well to the wide one. The interest of the CQW system is that the "escape mechanism" can be tuned by varying the barrier width, without affecting the sample quality. It is also possible, in principle, to study "on-resonance" as well as "off-resonance" conditions, where the ground state of the narrow-well would coincide (or not) in energy with the $n=2$ state of the wide well. As we shall show in the following, tunneling times can easily be varied from a few nanoseconds to a few picoseconds. Relaxation in the narrow well will then be influenced by this kind of internal time scale provided by the tunneling mechanism.

SAMPLE DESCRIPTION AND CHARACTERIZATION

We studied four GaAs/$Al_xGa_{1-x}As$ molecular-beam-epitaxy (MBE) -grown samples in which the narrow- (NW) and wide-well (WW) widths are kept in the same range (60 Å for the NW and 120 Å for the WW) and the tunnel-barrier widths L_b are 80, 60, 30, and 15 Å. The Al composition of the barriers is equal to about 26%. In the following we shall label the samples from their barrier width. Due to the well widths of our sample, there is no resonance between the energy levels of the two wells, and the energy separation from the electron ground state of the NW to the electron ground state of the WW is larger than one optical-phonon energy ($\hbar\omega_{LO}=36$ meV; see Fig. 1 for a schematic energy configuration of the CQW system). The spectra were recorded at 2 K, with an excitation density of about 100 W/cm^2.

Luminescence of such samples basically consists of two lines corresponding, respectively, to the NW and WW (see Fig. 1). As a result, from the increasing tunneling

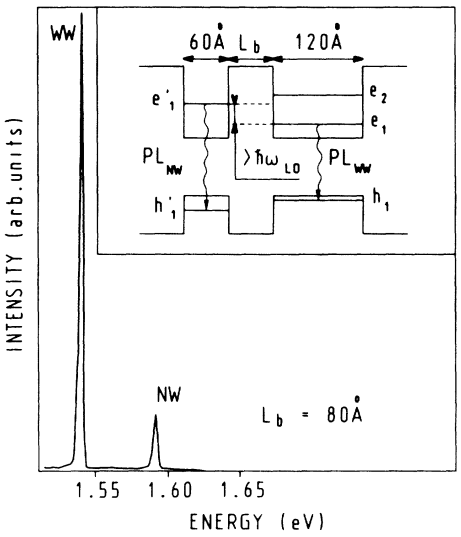

FIG. 1. Schematic energy diagram of the studied CQW systems (left), and typical luminescence spectrum for the case of an 80-Å barrier (right).

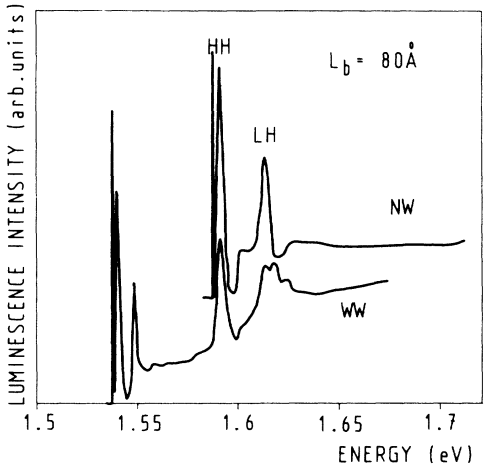

FIG. 2. PLE spectra detected on the WW luminescence line (WW) and on the NW luminescence line (NW) of a CQW with an 80-Å barrier.

probability from the NW to the WW, the intensity ratio I_{WW}/I_{NW} between these two lines increases when the barrier width decreases. This ratio, R, is reported in Table I. The luminescence of the WW shows a thin linewidth (about 1 meV) and the PLE detected on the WW indicates very little Stokes shift (less than 1 meV), indicating a rather high sample quality.

Time-resolved luminescence experiments have also been carried out on our samples by using both a synchroscan streak camera and an up-conversion setup with subpicosecond resolution similar to that described in Ref. 17. The decay times of the NW luminescence are also reported in Table I. Injected carrier densities for these measurements are of the order of 5×10^{10} cm^{-2} carriers per well, i.e., well above the residual p-type doping.

EXPERIMENTAL RESULTS

Figure 2 shows the PLE spectra detected on the two luminescence lines of the 80-Å sample. As usual for sufficiently thin barriers, the excitation of the WW line shows structures related to the NW.[18] This is direct evidence of the transfer of photoexcited carriers from the NW to the WW.[1,2] Similar PLE spectra are observed for the WW in all the samples studied hereafter. Very weak crossed transitions are also observed (involving electrons of one well recombining with holes in the other), especially at the highest excitation densities, but these will not be detailed in this paper.

In the following we shall only concentrate on the PLE spectra detected on the NW exciton line. For the $L_b=80$ Å sample the excitation spectrum of the NW shows the usual shape, typical of isolated quantum wells. The heavy- and light-hole exciton resonances (labeled HH and LH, respectively) are clearly marked. Although transfer occurs from the NW to the WW, this transfer has to be slower than the thermalization of the carriers. The exact mechanism for the formation of the exciton is still an open question; however, it is widely admitted that the overall time it takes for a photoexcited pair to relax and bind into an exciton is of the order of 200 ps.[19,20] Time-resolved experiments on the same sample indeed indicate transfer times to excess of 2000 ps (see Table I). For this last experiment to be possible, the temperature of the sample has to be raised to 80 K in order to get longer radiative lifetimes.

The results obtained for the 60-, 30-, and 15-Å samples are quite different: the intensity of the NW luminescence is now much weaker than that of the WW luminescence because of the increased transfer of the photoexcited carriers from the NW to the WW (see Table I). The NW luminescence is weak and shows several components [Fig. 3(a)]. The position of the NW heavy-hole–exciton resonance (observed in the excitation spectrum of the WW) corresponds to the high-energy component of the NW luminescence (1.591 eV). This is where we set the detection for the PLE measurement of the NW. We shall return to the shape of the NW luminescence later.

The PLE spectra of the NW line also drastically changes (see Fig. 4): it is necessary to keep in mind that in the three samples of Fig. 4, the intensity of the signal at the heavy-hole resonance is larger—by orders of magnitude–than the rest of the spectrum. All spectra show sharp oscillatory structures separated by 36 meV.

TABLE I. Summary of the behavior of the ratio R of the luminescence intensities of the WW and NW wells, and the measured decay times of the NW luminescence as a function of the barrier width L_b of the CQW system.

L_b (Å)	R ($\equiv I_{WW}/I_{NW}$)	τ (ps)
80	8	>2000
60	2000	260
30	8000	10
15	35 000	6

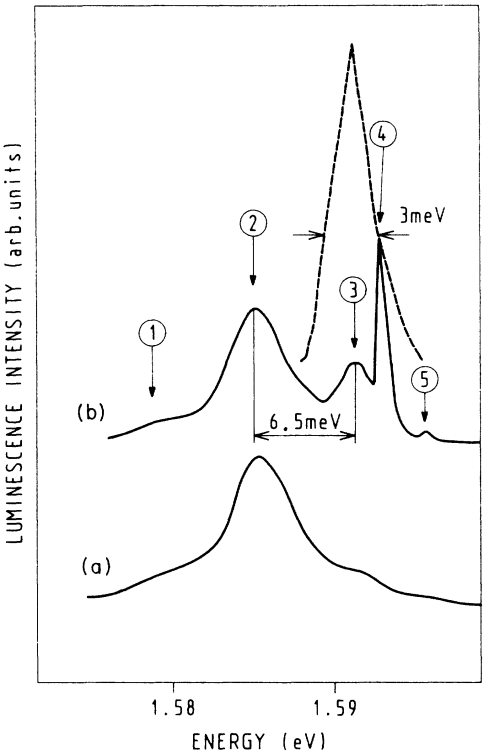

FIG. 3. (a) Spectrum of the NW luminescence of a CQW with a 30-Å barrier; (b) same luminescence line when the excitation is 72 meV above the high-energy component. Also shown as a dashed line is the variation of the intensity of peak 4 (attributed to Raman scattering or hot luminescence) when the excitation energy is scanned around 1.664 eV.

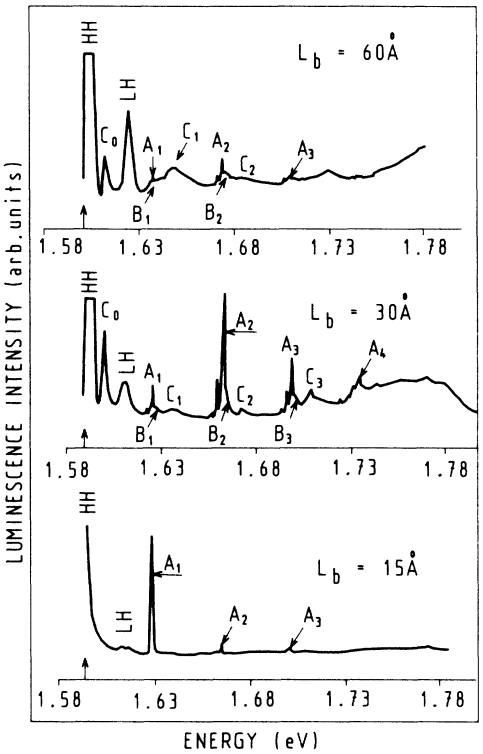

FIG. 4. PLE spectra detected on the NW luminescence line for three CQW's with 60-, 30-, and 15-Å barriers. The curves are slightly shifted so as to align the detection energies (indicated by an arrow). Note that the intensity of the HH- exciton resonance could go to 10 in the case of the 60-Å barrier and to 80 in the case of 30-Å barrier.

We shall first describe the results on the $L_b = 30$ Å sample, as they are sharper than in the other samples.

For the $L_b = 30$ Å the PLE spectrum of the NW line shows the usual heavy- and light-hole–exciton resonances, but also shows three series of marked oscillatory structures labeled A_n, B_n, and C_n. These three series exhibit a period of 36 meV; series A_n and B_n extrapolate to the heavy-hole–exciton line and series C_n extrapolates 9 meV higher (C_0 line). Structures A_n are composed of very sharp peaks standing on an asymmetrically broadened pedestal B_n. As n increases, replicas of the A_n series appear on the lower-energy side of the structure, separated by about 2.5 meV. Structures C_n are asymmetrically broadened and show no narrow peaks. When the detection energy is scanned across the HH PLE exciton resonance of the NW, the peaks A_n move together such that their series extrapolates directly to the detection energy with a 36-meV period. The structures B_n and C_n keep the same energy position. The intensity of each series is resonantly enhanced at this exciton resonance (see the dashed curve in Fig. 3). The intensity profile of the A_n and B_n resonances is quite peculiar, as the first replica is rather small, whereas the second is the most intense. The intensity of the following replica monotonously decreases.

Let us now return to the luminescence spectra of the NW (see Fig. 3). When nonresonantly excited, for example, by excitation at 2 eV, above the barriers, the spectrum of the narrow well corresponds to Fig. 3(a). The position of the excitonic line in PLE is 1.592 eV, corresponding to the highest-energy component (arrow 3). When the excitation energy E_{ex} is set about 72 meV above this structure ($1.592+0.072=1.664$ eV), sharp peaks appear superimposed on the luminescence spectrum [arrow 4, compare Figs. 3(a) and 3(b)]. The energy of the sharpest peak is exactly 72 meV below E_{ex} and follows it when E_{ex} is moved; this explains the behavior of the series A_n in the PLE spectra. A second peak appears in the luminescence spectrum about 2.5 meV above structure 4 (see arrow 5) and corresponds to the replica observed in PLE 2.5 meV below the A_2 peak (see Fig. 4). Moving the excitation energy around 1.664 eV results in a correlated displacement of the sharp peaks in the luminescence spectrum of Fig. 3(b). The intensity variation of the sharpest feature (arrow 4) is plotted as a dashed line in Fig. 3; this curve reproduces the excitonic absorption line quite well. A similar enhancement is shown, with lower intensity, by the small replica (arrow 5), and also by the broader structure (arrow 3).

If the PLE is now detected by setting the monochromator at 1.585 eV, on the strongest luminescence peak

(arrow 2), the sharp resonances A_n, B_n, and C_n do not appear any more. In the same way, in selective luminescence excited 72 meV above this line, no sharp structure is observed.

The luminescence and excitation spectra of the 60-Å sample show similar features, although they are less marked and broader than the structures in the 30-Å sample (see Fig. 4 for the PLE spectrum of the NW line).

The 15-Å sample gives a different picture: the spectrum is featureless except for the three sharp peaks at 36, 72, and 108 meV above the detection energy (Fig. 4). Those peaks follow the detection when it is scanned across the NW heavy-hole line and vanish when it is placed above or under this line. The background signal below these three peaks does not correspond to any luminescence from the NW, but to the high-energy tail of the WW luminescence, observed due to the very large amplification factor used in this experiment (the intensity ratio is 35 000; see Table I).

DISCUSSION

In order to interpret these observations, we shall study the relaxation of photocreated carriers in a CQW. For the sake of clarity the following discussion will be mainly qualitative. Some calculations leading to the quantitative estimates will, however, be used in the discussion. In our samples no resonance occurs between the quantized levels of the two wells, so that the wave functions are clearly located in one or the other well, and we can consider the CQW as two independent wells coupled through a barrier. Hence, "tunneling" from one well to the other necessarily means "assisted tunneling." First, we shall only consider electron tunneling, as (i) we are working in a low-density regime, (ii) the tunneling time of the holes is longer than that of electrons due to their larger effective mass, and (iii) relaxation of holes is also more rapid than electron relaxation, as they have less excess energy and interact more strongly with the phonons.

We shall try to order our discussion according to the following scheme: in the first subsection we show that the resonances we observed are not due to hot-electron relaxation, in the second we emphasize the basic features of hot-exciton relaxation, and in the third we give our full interpretation of the PLE or CQW's.

Hot-electron resonances?

In polar semiconductors the most efficient energy-relaxation channel for electrons is the emission of LO phonons. In quantum wells, intrasubband relaxation by LO-phonon emission occurs in a characteristic time of about 200 fs. As pointed out in Ref. 21, for a given relaxation channel, intrawell relaxation in CQW's is faster than interwell relaxation. Then, the electrons photocreated in the NW will all first relax down to the $[e_1, e_1+E_{\mathrm{LO}}]$ interval, where e_1 is the bottom of the NW first conduction band, by emitting the proper number of LO phonons. At this point, if the NW was not coupled to the WW, electrons would cool down to the band edge by acoustic-phonon emission, and bind with a hole into an exciton which would decay radiatively or nonradiatively. This roughly corresponds to the case of the $L_b=80$ Å sample, where the tunneling process is longer than 1 ns and can be neglected compared to relaxation processes. The times involved in the cooling of an electron-hole pair and its binding into an exciton are not perfectly documented up to now.[22,19,20] Cooling time depends on the excess energy to be lost by acoustic-phonon emission, and will be of the order of 100–200 ps. Formation of an exciton might be shorter [20 ps Ref. (20)], but, in any case, the subsequent cooling of the exciton also involves acoustic phonons, and the order of magnitude of the time will also be 100 ps.[19,20]

The key feature of our CQW is that, even in the $[e_1, e_1+\hbar\omega_{\mathrm{LO}}]$ interval, the electrons can still emit a LO phonon and tunnel to the WW (the NW band edge is more than one-LO-phonon energy higher than the WW band edge). If the time associated with this process is shorter than the binding of the electron and the hole into an exciton, most of the electrons of the NW will transfer to the WW during the last relaxation step. For sufficiently thin barriers, no NW luminescence would be expected if all excitons were to be formed from uncorrelated carriers. In the case of the 30-Å barrier, for example, the time decay of the NW luminescence is as short as 10 ps, i.e., shorter than the time required to bind an electron and a hole into an exciton. Even $k=0$ electrons will then tunnel before binding into an exciton.

As a consequence, the structures we observe cannot stem from an electron-relaxation process. This is confirmed by the fact that their energy separation is 36 meV, instead of 42 meV in the case of electron relaxation.[11,12]

Hot excitons

The 36-meV period of the observed resonances suggest that they are related to "hot"-exciton relaxation:[11,13] Since such excitons have a large **k** vector, they can only be created by indirect absorption of light involving a large-q phonon. Of course, such indirect absorption has a weak oscillator strength. It is only evidenced in our experiments since the contribution of free-electron–hole pairs created by direct absorption is completely washed out (remember the large intensity ratios between the luminescence of the two wells). Like "hot" electrons, "hot" excitons with a kinetic energy in excess of E_{LO} (from now on, we take the origin of the energies at the bottom of the exciton 1s subband) will mainly interact with LO phonons: upon LO-phonon emission they can be scattered into their own band, to another band, or to the continuum. We shall only consider intraband scattering and scattering into the continuum (dissociation) for 1s excitons.

To compute the indirect-absorption coefficient (as well as the scattering and dissociation times), the electron–LO-phonon interaction is included to the second order (emission of one phonon only will be considered). The exciton wave functions and the exciton-phonon interaction are written as in Ref. 23 (only the Fröhlich interaction is considered). We do not treat the

continuum as interacting electron-hole pairs, but rather as plane waves. A complete treatment (taking the correlation of the electron-hole pairs of the continuum into account) of the indirect excitonic absorption can be found in Ref. 24 for the three-dimensional (3D) case. The case of 2D phonon-assisted indirect absorption, with a correct treatment of the continuum states, can be found in Ref. 25. We used the following parameters: electron mass $m_e/m=0.07$, and hole mass $m_h/m=0.4$ in units of the free-electron mass.

The arbitrarily normalized absorption coefficient (indirect creation of a $1s$ exciton with LO-phonon emission) is shown in Fig. 5 for a 60-Å well. Creation of hot excitons with the participation of $q=0$ phonons is then forbidden. The large enhancement of the phonon-assisted absorption just above E_{LO} could just be an artifact of our model for the phonons as it stems from our allowance for phonons with zero transverse wave vector and would not appear as strongly if we had used confined phonons. In the case of confined-phonon modes, the maximum of the absorption probability will nevertheless be reached between E_{LO} and $2E_{LO}$, but would be less pronounced. As the exact shape of the absorption curve strongly depends on the chosen phonon model, we have not attempted a quantitative comparison with the experiment. We shall only retain the following characteristics: indirect absorption is forbidden at E_{LO}, reaches its maximum between E_{LO} and $2E_{LO}$, and becomes negligible for energies larger than a few E_{LO}. The case of $2s$ excitons is different and does not lead to any interdiction of the $q=0$ process.[26]

The inverse-scattering and dissociation times are shown in Fig. 6 for the same well width. We find that the scattering $(1/W_{scatt})$ and dissociation $(1/W_{dissoc})$ times for an exciton of a given energy are on a subpicosecond time scale and of the same order of magnitude. A similar

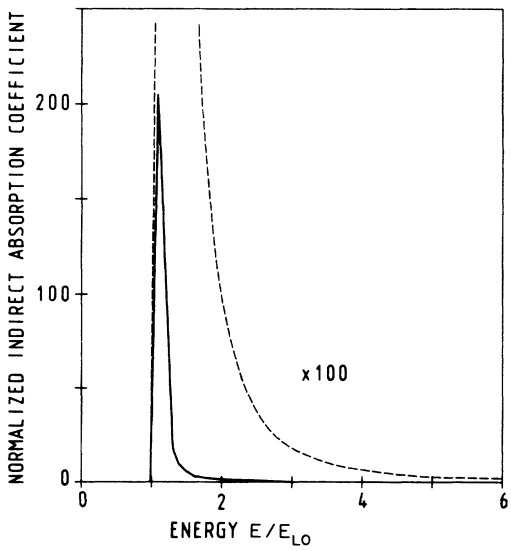

FIG. 5. Arbitrarily normalized $[a(2E_{LO})=1]$ indirect-absorption coefficient for a 60-Å-wide quantum well. The origin of the energies is at the bottom of the $1s$ exciton band.

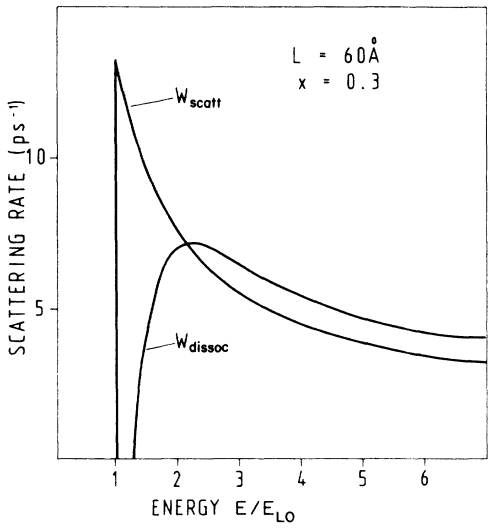

FIG. 6. Scattering and dissociation rates for $1s$ excitons in a 60-Å-wide well. The origin of the energies is at the bottom of the $1s$ exciton band.

result was obtained for bulk CdS (Ref. 13), and a detailed study of the dissociation and scattering times for hot 3D excitons can be found in Ref. 27 and 28.

Our results imply that a significant proportion of excitons with a kinetic energy in excess of E_{LO} will reach the $[0,E_{LO}]$ interval by LO-phonon emission, before being dissociated or transferred to the WW. This multiphonon-cascade process is described in detail in Ref. 11 for the 3D case, but in two dimensions the basics are unchanged.

In the $[0,E_{LO}]$ interval, excitons of an isolated well can only cool down by emission of acoustic phonons or ionize by acoustic-phonon emission and impurity scattering. At this point, the times involved are so long that we cannot ignore their possible tunneling to the WW for the case of the CQW system. If this tunneling time is short compared to the cooling time, excitons with nonzero kinetic energy will not be able to relax their energy completely and give rise to luminescence. In this case luminescence from the NW only stems from those excitons which can avoid the last slow relaxation step, i.e., excitons whose kinetic energy is an integer multiple of E_{LO}. Resonances are then expected at these energies in excitation spectra. The intensity of the nth resonance varies as

$$I_n \propto a(nE_{LO}) \prod_{m=1}^{n-1} \frac{W_{scatt}(mE_{LO})}{W_{tot}(mE_{LO})} , \tag{1}$$

where $W_{tot}(E)$ is the inverse total lifetime of an exciton with kinetic energy E.[29] As a rough approximation, we can write

$$W_{tot}(E)=W_{scatt}(E)+W_{dissoc}(E) , \tag{2}$$

neglecting the contribution to the total lifetime of the scattering to excited levels.

It should be noted that in the above cascade model the steady-state distribution at the exciton band edge is

thermalized.[11] Two more scattering mechanisms should be added to this model.

(i) Multiphonon resonant Raman scattering, well documented in three dimensions.[30,31]

(ii) Nonthermalized ("hot") luminescence: if the average thermalization time is greater than or comparable to the exciton lifetime at the band edge we must include the possibility of an additional nonthermalized exciton distribution at an integer multiple of E_{LO} below the excitation energy.

Whether Raman scattering and hot luminescence can be distinguished in steady-state experiments is still not clear.[32,33] They both lead to sharp peaks at integer multiples of E_{LO} above the detection energy in excitation spectra. As the two processes involve the same intermediate states as the "standard" multiphonon-cascade mode, a golden-rule approach shows that the intensity of the peaks varies according to (1) in both cases.

Full interpretation

We can now give our interpretation of the PLE spectra presented above. In the 80-Å sample the barrier is thick enough so that the contribution of the indirect absorption cannot be resolved from the contribution of the nontunneling electrons, and the PLE spectrum has its usual shape.

In the $L_b = 60$ and 30 Å samples, the coupling between the wells is strong enough to wash out the contribution of the electrons created by direct absorption. This is possible not only because of the thin barriers but also because of the energy difference between the ground states (on another sample with a 50-Å barrier, but where the difference between the ground states was less than E_{LO}, the excitation of the NW luminescence only shows structures typical of isolated wells).

The series A_n is attributed to multiphonon resonant Raman scattering or "hot" luminescence; the fact that they follow the detection position, their intensity resonance at the NW HH-exciton energy, and the very narrow linewidths confirm this. The distribution of the intensity of the A_n lines is also in agreement with this interpretation: The A_1 transition is almost forbidden. The replica 2.5 meV below the main line corresponds to the GaAs-type phonon mode of the $Al_xGa_{1-x}As$ barriers. It should be noted that in our model the A_1 peak (corresponding to indirect absorption assisted by one LO phonon of zero momentum) is forbidden; taking into account the polariton effect in the final state would lift this selection rule as the excitons giving rise to luminescence have a very small but nonzero momentum. Similar phenomena have been observed and interpreted in the same terms by Planel *et al.*[13] in bulk CdS: in, admittedly, "surface-polluted" samples the uncorrelated electrons were trapped by very efficient nonradiative centers, and multiphonon cascades were observed in the excitation spectra of both free and impurity-bound excitons (also see Ref. 34). In our case the "trapping" of the electrons can be controlled by the barrier width and is by no means related to a poor quality of the samples.

The series B_n is attributed to a similar multiphonon cascade of excitons terminating on a thermalized distribution of excitons at the band edge. Those resonances are broadened on their high-energy side by the participation of acoustic phonons in the last thermalization step.

Series C_n is attributed to the equivalent cascade terminating on excited bound states of the exciton. It should be noted that in our interpretation series C_n cannot extrapolate directly to the electron band edge because the resulting uncorrelated zero-kinetic-energy electrons would tunnel to the WW rather than bind with a hole into an exciton and contribute to the NW luminescence. Noting that the binding energy of the $2s$ exciton is about $\frac{1}{10}$ of the binding energy of the $1s$ exciton, and mostly attributing the C_0 resonance to the $2s$ exciton, we obtain a $1s$ binding energy of 10 meV in good agreement with theoretical estimates.[35] Confirmation of this interpretation comes from the fact that the C_1 transition is not forbidden, contrary to the case of $1s$ excitons.[26]

These assignments also explain the features of the NW selective luminescence spectra (see Fig. 3). Resonant Raman scattering (RRS) and "hot" luminescence probe the $k \sim 0$ free-exciton density of states and may yield to sharp peaks only when the exciting energy is an integer multiple of E_{LO} above the free-exciton line. The envelope of the intensity of the observed peaks coincides both with the NW heavy-line–exciton resonance (detected in the WW PLE), and with the high-energy component of the NW luminescence.

Therefore we assign the high-energy component of the NW luminescence (1.591 eV) to free excitons. When PLE is performed on the low-energy component of the luminescence line (1.585 eV), no RRS peaks are detected. This leads us to attribute this low-energy component to localized excitons: selection rules described in the second subsection do not hold for localized excitons. The measured localization energy of 6.5 meV is in correct agreement with the binding energy of an exciton localized by a one-monolayer terrace of at least 100 Å radius.[36] As very few excitons are created because of the tunneling processes discussed above, the trapping centers never get saturated and this low-energy component may dominate the spectrum.

Let us finally note that time-resolved study of the resonant peaks which appear in luminescence might help us to distinguish between resonant Raman scattering and "hot" luminescence.[34]

The results obtained on the 15-Å sample are in apparent contradiction with the above interpretation. This can be resolved if we note that for a 15-Å barrier the tunneling time of the excitons becomes short compared to its radiative lifetime, so that resonances due to cascades terminating on real exciton states (thermalized or not) are also washed out of the spectrum. This explains the disappearance of the B_n and C_n series in the PLE spectrum and the absence of luminescence from the NW. The shape of the envelope of the Raman lines will be modified for the same reason; the inverse total lifetime should be corrected:

$$W_{tot}(E) = W_{scatt}(E) + W_{dissoc}(E) + W_{tunnel}(E) ,$$

where W_{tunnel} takes the hole tunneling into account. If W_{tunnel} becomes larger than $W_{\text{scatt}}+W_{\text{dissoc}}$, the intensity I_n roughly decreases as $(1/W_{\text{tunnel}})^n$, which is indeed in qualitative agreement with the experiment.

A similar phenomenon has been observed and interpreted by Kleinman *et al.*[37] in various single or multiple quantum wells. In this case probable trapping of the uncorrelated electrons (resulting in an admitted very weak luminescence efficiency) made the observation of resonant-Raman-scattering-related lines possible.

CONCLUSIONS

Previous studies invoked "escape mechanisms" such as trapping by nonradiative centers of poor sample quality and flowing of carriers to the substrate or the surface due to efficient transport to explain the observation of RRS and hot-exciton resonances in the excitation spectra. Such mechanisms could not be easily controlled or quantitatively analyzed. In the CQW system the ability to vary the electron and hole tunneling times from the NW to the WW enabled us to study in detail the influence of a tunable "escape mechanism" on PLE spectra.

ACKNOWLEDGMENTS

We wish to thank R. Planel, C. Benoit à la Guillaume, G. Bastard, and B. Lambert for enlightening discussions.

[1]R. Sauer, K. Thonke, and W. T. Tseng, Phys. Rev. Lett. **61**, 609 (1988).
[2]B. Deveaud, A. Chomette, A. Regreny, J. L. Oudar, D. Hulin, and A. Antonetti, in *High Speed Electronics,* edited by B. Källback and H. Beneking (Springer-Verlag, Berlin, 1986), p. 101.
[3]Y. Tokuda, K. Kanamoto, N. Tsukuda, and T. Nakayama, J. Appl. Phys. **65**, 2168 (1989).
[4]Y. Tokuda, K. Kanamoto, N. Tsukuda, and T. Nakayama, Appl. Phys. Lett. **54**, 1232 (1989).
[5]J. E. Golub, P. F. Liao, D. J. Eilenberger, J. P. Harbinson, L. T. Florez, and Y. Prior, Appl. Phys. Lett. **53**, 2584 (1988).
[6]T. B. Norris, N. Vodjani, B. Vinter, C. Weisbuch, and G. A. Mourou, Phys. Rev. B **40**, 1392 (1989).
[7]D. Y. Oberli, J. Shah, T. C. Damen, D. A. B. Miller, and C. W. Tu, Bull. Am. Phys. Soc. **34**, 501 (1989), and unpublished.
[8]G. W. Alexander, W. W. Rühle, R. Sauer, W. T. Tsang, K. Ploog, and K. Köhler (unpublished).
[9]N. Sawaki, R. A. Höpfel, E. Gornik, and H. Kano (unpublished).
[10]H. Q. Le, J. J. Zayhowski, and W. D. Goodhue, Appl. Phys. Lett. **50**, 1518 (1987).
[11]S. S. Permogorov, Phys. Status Solidi B **68**, 9 (1975).
[12]C. Weisbuch, Solid-State Electron. **21**, 179 (1978).
[13]R. Planel, A. Bonot, and C. Benoit à la Guillaume, Phys. Status Solidi B **58**, 251 (1973).
[14]E. Gross, S. Permogorov, V. Travnikov, and A. Selkin, J. Phys. Chem. Solids **31**, 2595 (1970).
[15]A. Chomette, B. Lambert, B. Deveaud, F. Clérot, and H. W. Liu, and A. Regreny, Semicond. Sci. Technol. **3**, 351 (1988).
[16]K. Moore, G. Duggan, P. Dawson, and C. T. Foxon, Superlatt. Microstruct. **5**, 481 (1989).
[17]J. Shah, T. C. Damen, B. Deveaud, and D. Block, Appl. Phys. Lett. **50**, 1307 (1987).
[18]H. W. Liu, R. Ferreira, G. Bastard, C. Delalande, J. F. Palmier, and B. Etienne, Appl. Phys. Lett. **54**, 2082 (1989).
[19]J. I. Kusano, Y. Segawa, Y. Aoyagi, S. Namba, and H. Okamoto, Phys. Rev. B **40**, 1685 (1989).
[20]T. C. Damen, J. Shah, D. Y. Oberli, D. S. Chemla, J. E. Cunningham, and J. M. Kuo (private communication).
[21]R. Ferreira and G. Bastard, Phys. Rev. B **40**, 1074 (1989).
[22]R. Hoger, E. O. Göbel, J. Kuhl, K. Ploog, and H. J. Queiser, J. Phys. C **17**, L905 (1984).
[23]S. Rudin and T. L. Reinecke, Solid State Commun. **68**, 739 (1988).
[24]C. Trallero Giner, I. G. Lang, and S. T. Pavlov, Phys. Status Solidi B **100**, 631 (1980).
[25]S. Rudin and T. L. Reinecke, Phys. Rev. B **39**, 8488 (1989).
[26]A. Bonot, R. Planel, and C. Benoit à la Guillaume, Solid State Commun. **13**, 733 (1973).
[27]K. A. Aristova, C. Trallero Giner, I. G. Lang, and S. T. Pavlov, Phys. Status Solidi B **85**, 351 (1978).
[28]C. Trallero Giner, O. Soto-Longo Costa, I. G. Lang, and S. T. Pavlov, Fiz. Tverd. Tela (Leningrad) **24**, 2724 (1982) [Sov. Phys.—Solid State **24**, 1544 (1982)].
[29]E. L. Ivchenko, I. G. Lang, and S. T. Pavlov, Fiz. Tverd. Tela (Leningrad) **19**, 1227 (1977) [Sov. Phys.—Solid State **19**, 718 (1977)].
[30]*Light Scattering in Solids,* edited by M. Cardona (Springer-Verlag, New York, 1975).
[31]A. V. Goltsev, I. G. Lang, S. T. Pavlov, and M. F. Bryzhina, J. Phys. C **16**, 4221 (1983).
[32]M. V. Klein, Phys. Rev. B **8**, 919 (1973).
[33]Y. R. Shen, Phys. Rev. B **9**, 622 (1974).
[34]A. Nakamura and C. Weisbuch, Solid-State Electron. **21**, 1331 (1978).
[35]G. D. Sanders and Y. C. Chang, Phys. Rev. B **32**, 5517 (1985).
[36]G. Bastard, *Wave Mechanics Applied to Semiconductor Heterostructures* (Les Editions de Physique, Paris, 1989).
[37]D. A. Kleinman, R. C. Miller, and A. C. Gossard, Phys. Rev. B **35**, 664 (1987).